https://doi.org/10.5194/essd-2026-723
Preprint. Discussion started: 2 November 2026
© Author(s) 2026. CC BY 4.0 License.



Open Access Earth System Science Data Discussions

Imaging the Ross Ice Streams of West Antarctica using active source seismology

Huw Horgan[1,2,3], Andrew Gorman[4], J. Paul Winberry[5], Sridhar Anandakrishnan[6], Howard Conway[7], Gavin Dunbar[3], Tina van de Flierdt[8], Denise Kulhanek[9,10], Richard Levy[11,3], Molly Patterson[10], and Ilaria Santin[1,2]

[1]Laboratory of Hydraulics, Hydrology and Glaciology (VAW), ETH Zurich, Zurich, Switzerland
[2]Swiss Federal Institute for Forest, Snow and Landscape Research (WSL), bâtiment ALPOLE, Sion, Switzerland
[3]Antarctic Research Centre, Victoria University of Wellington, Wellington, New Zealand
[4]Department of Geology, University of Otago, Dunedin, New Zealand
[5]Department of Geological Sciences, Central Washington University, Ellensburg, WA, USA
[6]Department of Geosciences, Pennsylvania State University, University Park, PA, USA
[7]Earth and Space Sciences, University of Washington, Seattle, WA, USA
[8]Department of Earth Science and Engineering, Imperial College London, London, UK
[9]Institute of Geosciences, Christian-Albrechts-Universität zu Kiel, Kiel, Germany
[10]Department of Earth Sciences, Binghamton University, Binghamton, NY, USA
[11]Earth Sciences New Zealand, Lower Hutt, New Zealand

Correspondence: Huw Horgan (huw.horgan@slf.ch)

Abstract. Beneath Earth's ice sheets the underlying geology both regulates the flow of the overriding ice and archives its history. Investigating this hidden environment from the ice sheet surface requires remote geophysical methods. Active source seismology has proven an effective method capable of investigating ice sheet internal structure, the ice–bed interface, subglacial water bodies, and the underlying geology. Here we present a compilation of published and unpublished active source seismic data from the Ross Ice Streams of West Antarctica (https://doi.org/10.5281/zenodo.19068423, Horgan et al., 2026). The data sample a range of glaciological environments from subglacial lakes to pinning points. Despite the lack of geographic overlap, and sparse spatial coverage, the following conclusions can be drawn. (1) Subglacial geology, specifically the presence of a substrate smoothed and mantled by sediment, correlates with regions of present or past rapid ice flow. (2) Subglacial water is observed in a range of glaciological settings including the onset region, beneath streaming ice, and close to the grounding zone. (3) Pinning points and sticky spots manifest in a range of substrate types, from relatively smooth and sediment covered to relatively rough acoustic basement. (4) The Siple and Gould Coast grounding zone exhibits a shallow sub-ice-shelf ocean cavity, with some evidence of active sedimentation, but none of the asymmetric grounding zone wedge deposits thought to stabilise grounding zone retreat. Recent geological coring on Crary Ice Rise highlights both the utility of existing seismic data, and the need for more extensive surveying. Such surveying would aid the interpretation of the geological record, help locate additional palaeoclimate drilling targets and allow for improved calibration of geophysical methods used to constrain glaciological properties and processes.

https://doi.org/10.5194/essd-2026-723
Preprint. Discussion started: 2 November 2026
© Author(s) 2026. CC BY 4.0 License.



Open Access Earth System Science Data Discussions

1 Introduction

Since their inception, Antarctica's ice sheets have exerted a major control on Earth's surface through the modulation of sea level (Miller et al., 2005). Antarctica's modern ice sheets contain the equivalent of approximately 58 m of global sea level (Fretwell et al., 2013). Between 1992 and 2017, mass loss from these ice sheets exceeded mass gain by 2720 ± 1390 billion tonnes of ice resulting in 7.6 ± 3.9 mm of sea level rise (Shepherd et al., 2018; Otosaka et al., 2023). While modern rates of mass loss are significant, there is also evidence of major changes of Antarctica's ice sheets in the past. Far-field records of relative and global sea level during marine isotope stage (MIS) 5e and MIS 11 indicate the potential for multi-metre contributions from Antarctica (e.g. Hearty et al., 2007), however, the magnitude of this contribution remains uncertain in part due to the absence of complementary near field constraints on ice volume (Dutton et al., 2015). Cosmogenic exposure records retrieved from the limited rock exposures inland in West Antarctica document several hundred metres of ice sheet thinning since the last glacial maximum (e.g. Stutz et al., 2023) and geomorphic evidence observed on the sea bed records complex patterns of advance and retreat (e.g. Simkins et al., 2018). Numerical models show ice histories with significant regional variations (Goelzer et al., 2016; Golledge et al., 2021) and unsurprisingly those constrained by observations best fit observed thinning histories (e.g. Spector et al., 2019).

The presence and variability of glaciers, ice sheets, and ice shelves leaves an imprint on the geological record. One means by which this record can be examined is through the use of active source seismology, which has been used to constrain both the long-term history and controlling processes occurring beneath the ice sheets (e.g. Cooper et al., 1993; Bart and Owolana, 2012; Hofstede et al., 2021). On ice sheets, oversnow active source surveying uses terrestrial seismic surveying methods adapted for the cryosphere and has a long history including the first measurements of the Greenland Ice Sheet's thickness in 1929 (Robin and Swithinbank, 1987). Oversnow seismic surveying is slower than its marine counterpart with seismic sources typically drilled to depths of 20–30 m (Smith, 2007) and geophones shallowly buried and often shifted between every shot. This has resulted in sparse oversnow seismic data coverage compared to in the marine environment. Oversnow seismic data are also typically low-fold (few repeat measurements made at the same location), resulting in low signal-to-noise ratios, when compared to marine data. More recently, oversnow vibroseis sources have been implemented in polar regions (e.g. Eisen et al., 2015; Zeising et al., 2026). While this technology is capable of acquiring medium-fold profile data at a rate approximately an order of magnitude faster than explosive source methods, its coverage so far remains geographically limited due to the expense and logistical footprint. Despite the relatively low quantities and quality of oversnow seismic data from polar regions these data have proven valuable for glaciological studies (Blankenship et al., 1986; Anandakrishnan et al., 1998; Hofstede et al., 2021; Luthra et al., 2017), characterising water bodies beneath ice sheets and ice shelves (e.g. Kapitsa et al., 1996; Bentley, 1990; Brisbourne et al., 2020), and for locating and contextualising valuable direct access drilling sites (Woodward et al., 2010; Patterson et al., 2022).

https://doi.org/10.5194/essd-2026-723
Preprint. Discussion started: 2 November 2026
© Author(s) 2026. CC BY 4.0 License.



Open Access Earth System Science Data Discussions

Here we present a compilation of oversnow active source seismic data from the Ross Ice Streams of West Antarctica (Fig. 1). This region includes the ice streams of the Siple and Gould coasts that drain the West Antarctic Ice Sheet and feed the Ross Ice Shelf. The seismic surveys we present sample ice streams, an ice rise, grounding zones, the sub-ice-shelf cavity and a subglacial drainage channel. The surveys lack geographic overlap but where possible we identify common attributes. Our efforts and the associated data release are motivated by the need to improve knowledge of processes beneath ice sheets and ice shelves, and to aid interpretation of palaeostratigraphic drilling records from the Siple Coast (Calkin et al., 2024; Patterson et al., 2022). We focus here on data attributes useful for seismic imaging and interpretation, but note the value of quantitative data analysis and reference these studies where possible. We begin by presenting a brief review of oversnow seismic methods in Section 2. In Section 3 both published and previously unpublished oversnow seismic profiles are presented. In Section 4 we group common glaciological settings and discuss the observations and their limitations. Section 5 presents our conclusions and an outlook.

2 Oversnow seismic methods

The oversnow active source seismic methods reported here all used an explosive energy source buried at depth. Upon detonation, explosive energy propagates and reflects off of contrasts in elastic properties. This reflected energy is then recorded at the surface on linear arrays of geophones (receivers) and the time series of reflectivity is used to create an image of the subsurface (Fig. 2a, b). Repeated imaging of the same point on the subsurface, ideally using shot and receiver pairs spaced at different offsets, allows the signal-to-noise ratio to be improved and enables additional processing approaches to further enhance subsurface imaging. The proportion of energy reflected at an interface (R) for a normal incidence ray path depends on the contrast in acoustic impedance ($Z = \rho v$, where ρ denotes density and v denotes velocity) and can be used to estimate the nature of the substrate (Smith, 2007). Reflectivity varies with angle of incidence ($R(\theta)$), providing additional information with which the nature of the substrate can be determined (e.g. Peters et al., 2008; Holland and Anandakrishnan, 2009). At normal incidence, an increase in acoustic impedance results in a positive polarity return and a decrease in a negative polarity return. The expected reflection amplitudes for ice overlying water, consolidated till, unconsolidated till, and bedrock are distinct, allowing seismic methods to differentiate between common bed types (Smith, 2007). These attributes are referenced in Section 3 to aid our interpretation.

Survey geometries (the placement of sources and receivers) in polar environments are often a compromise between diverse objectives including imaging the subsurface, amplitude analysis of the return from the base of the ice to determine bed properties, and survey coverage. Seismic surveying for glaciology is typically interested in the nature of the basal interface, while surveying for palaeostratigraphic drilling is more interested in resolving seismic stratigraphy and structure at greater depths. A common factor between all the oversnow surveys presented here is the relatively low fold (repeat observations of the same point), which results from a desire for a survey coverage of tens of kilometres per field season. This results in relatively poor imaging below the base of the ice and fewer processing options when compared with higher-fold data. The use of explosive sources buried at approximately 20–30 m also introduces a prominent short-path multiple (often termed a shot-ghost), which needs to be considered during interpretation (Fig. 2a,b).

https://doi.org/10.5194/essd-2026-723
Preprint. Discussion started: 2 November 2026
© Author(s) 2026. CC BY 4.0 License.

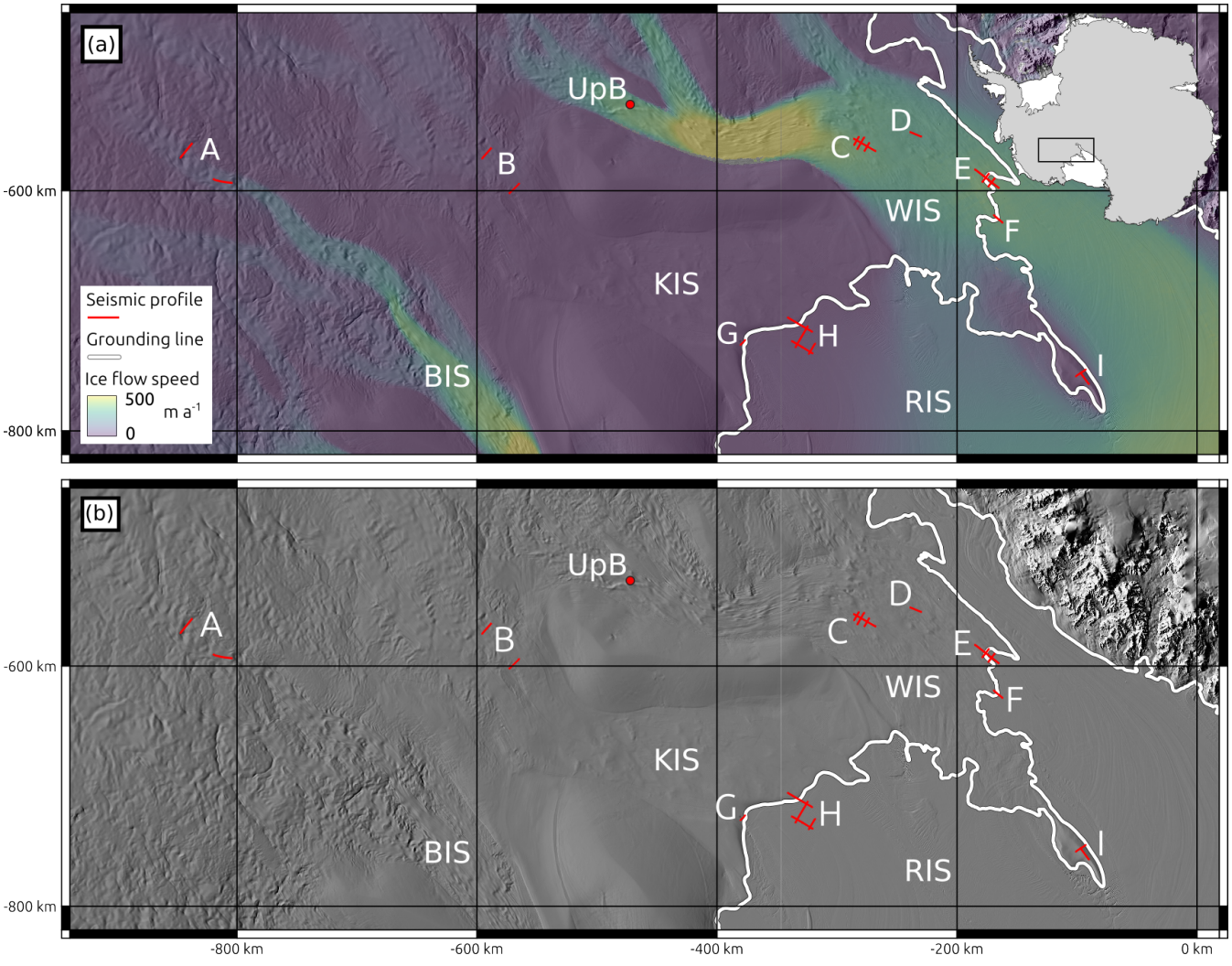


Figure 1. (a) Seismic survey locations A–I with profiles shown in red. Locations A–I refer to the panels (a)–(i) in Fig. 3. Imagery shows ice flow velocity (Rignot et al., 2011) at 30 % opacity overlain on hillshade of ice surface elevation (Howat et al., 2019). The grounding line separating grounded ice from the Ross Ice Shelf (RIS) is shown in white (Depoorter et al., 2013). BIS denotes Bindschadler Ice Stream, KIS denotes Kamb Ice Stream, and WIS denotes Whillans Ice Stream. UpB denotes the location of the seismic surveying reported in Blankenship et al. (1986) and Rooney et al. (1987). The inset in upper right shows location of the main figure. (b) The same survey locations as above underlain with elevation hillshade from the Reference Elevation Model of Antarctica (REMA) (Howat et al., 2019). The map projection is polar stereographic (EPSG:3031).

https://doi.org/10.5194/essd-2026-723
Preprint. Discussion started: 2 November 2026
© Author(s) 2026. CC BY 4.0 License.



Open Access Earth System Science Data Discussions

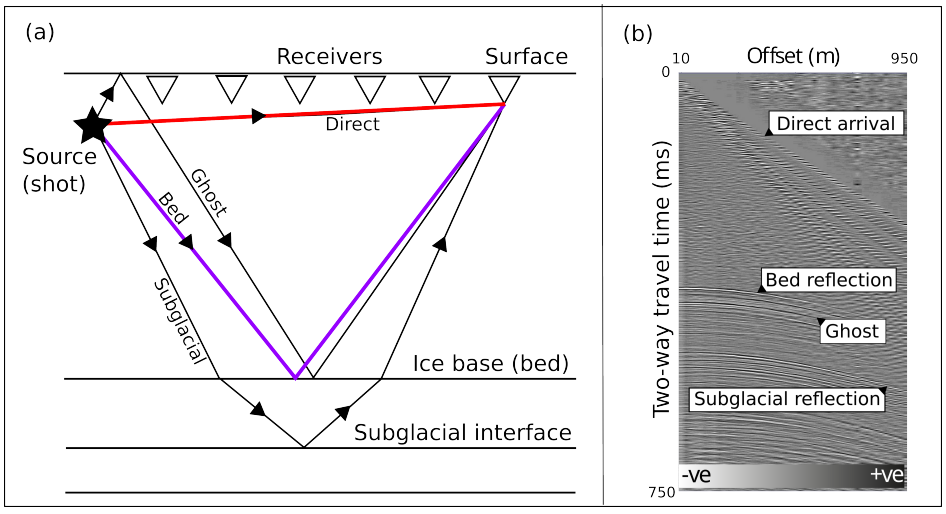


Figure 2. (a) Seismic reflection acquisition geometry showing source and receivers and common ray paths. (b) An example shot record of ice overlying water and sediments annotated with events resulting from common ray paths shown in (a).

Table 1. Active source seismic surveys presented here. Survey names include a 3-letter survey code followed by a 4-digit survey season (e.g. OND0203 is the OND survey from the 2002–2003 austral summer season). Line names are in keeping with original field acquisition notes and existing publications. In the location field, BIS denotes Bindschadler Ice Stream, KIS denotes Kamb Ice Stream, WIS denotes Whillans Ice Stream, and CIR denotes Crary Ice Rise. Alongside the references in the table, we note that Peters et al. (2006) present a seismic refraction investigation of OND0203 line DT1, and reflection velocity analysis of OND0203 line DL1.

Survey	Line	Fold	Reference	Location (Figs. 1, 3)
OND0203	DT1	4-fold	Horgan et al. (2011)	BIS (A)
OND0203	DL1	4-fold	Peters et al. (2007); Horgan et al. (2011)	BIS (A)
OND0203	CT1	4-fold	Luthra et al. (2017)	KIS (B)
OND0203	CT2	4-fold	Unpublished	KIS (B)
SLW1011	L1–L4	2,4-fold	Horgan et al. (2012)	WIS (C)
WIS1112	LLine	4-fold	Luthra et al. (2016)	WIS (D)
GLI1112	L1, X1, X2	4-fold	Horgan et al. (2013, 2021)	WIS (E)
GLI1112	L2	4-fold	Horgan et al. (2013, 2021)	WIS (F)
KAM1516	X1	2-fold	Unpublished	KIS (G)
KAM1516	L1	2-fold	Horgan et al. (2017)	KIS (H)
KAM1819	1, 2	2-fold	Unpublished	KIS (H)
KAM1920	2x, 3	2-fold	Unpublished	KIS (H)
CIR1516	TLine	2-fold	Patterson et al. (2022)	CIR (I)
CIR1516	LLine	2-fold	Unpublished	CIR (I)

https://doi.org/10.5194/essd-2026-723
Preprint. Discussion started: 2 November 2026
© Author(s) 2026. CC BY 4.0 License.



Open Access Earth System Science Data Discussions

3 Results

In this section we present the surveys in the order shown in Figs. 1 and 3. We present processed data, known in active source seismology as stacked data, with a typical processing sequence shown in Table A1. We begin with a description of the glaciological setting of each survey followed by a brief description of each data set that focuses on the basal return, subglacial structure, and other notable characteristics. All profiles are shown with upstream oriented to the left in the case of along flow profiles, and downstream into the page in the case of transverse profiles. We use true left and true right to indicate left and right when looking in the direction of flow. Surveys and lines are referred to by the names listed in Table 1.

3.1 Onset of Bindschadler Ice Stream

The onset region is defined as the transition between ice-sheet flow dominated by deformation and ice-stream flow dominated by basal sliding (e.g. Bindschadler et al., 2000). OND0203 surveyed the onset region of Bindschadler Ice Stream. Two seismic reflection profiles were acquired, one transverse to ice flow (line DT1) crossing onto the faster flowing ice stream, and one longitudinal profile in the centre of the ice stream (line DL1) (Fig. 3a). Line DT1 (Fig. 4) exhibits a high-amplitude bed return with mixed polarity and no evidence of subglacial sedimentary structure. Abundant reflectivity is observed within the ice, which is thought to result from abrupt contrasts in ice crystal orientation fabric (Horgan et al., 2011). The longitudinal line (DL1, Fig. 5) begins approximately 30 km downstream and exhibits a smooth, mostly negative polarity, high-amplitude basal return. Basal highs are observed at either end of the profile and englacial reflectivity is again observed in the overriding ice, although not to the same extent as in the transverse profile.

3.2 Onset of Kamb Ice Stream

OND0203 also acquired two transverse profiles upstream of the stagnant trunk of Kamb Ice Stream where Rignot et al. (2011) indicate surface velocities of approximately 20 m a^{-1} (Fig. 3b). Line CT2 (Fig. 6) displays a high-amplitude positive polarity bed return, with generally smooth bed topography. The presence of an unconsolidated sedimentary body on the true-right of the profile is indicated by a low-amplitude basal return. The downstream profile (CT1, Fig. 7), which was previously reported by Luthra et al. (2017), crosses onto a feature prominent in surface imagery (e.g. Scambos et al., 2007) and elevation data (e.g. Howat et al., 2019). The basal return is mostly high amplitude and positive polarity. Beneath the surface feature, a basal high exhibits mixed polarity. Adjacent to the basal high, the basal return is high amplitude and positive. No subglacial reflectivity indicative of sedimentary stratigraphy is apparent on or off the basal high.

3.3 Whillans Subglacial Lake and Sticky Spot

Whillans Subglacial Lake is an active lake beneath Whillans Ice Stream (Fricker et al., 2007; Smith et al., 2009). Oversnow geophysical surveying at Lake Whillans (Fig. 3c) characterised the lake and identified a direct access drilling target (Horgan et al., 2012; Christianson et al., 2012). The basal return at Lake Whillans consists of high-amplitude, negative-polarity waveforms, consistent with water at the bed. Ice over water reflectivity is observed beyond the active lake boundary (Fricker et al.,

https://doi.org/10.5194/essd-2026-723
Preprint. Discussion started: 2 November 2026
© Author(s) 2026. CC BY 4.0 License.

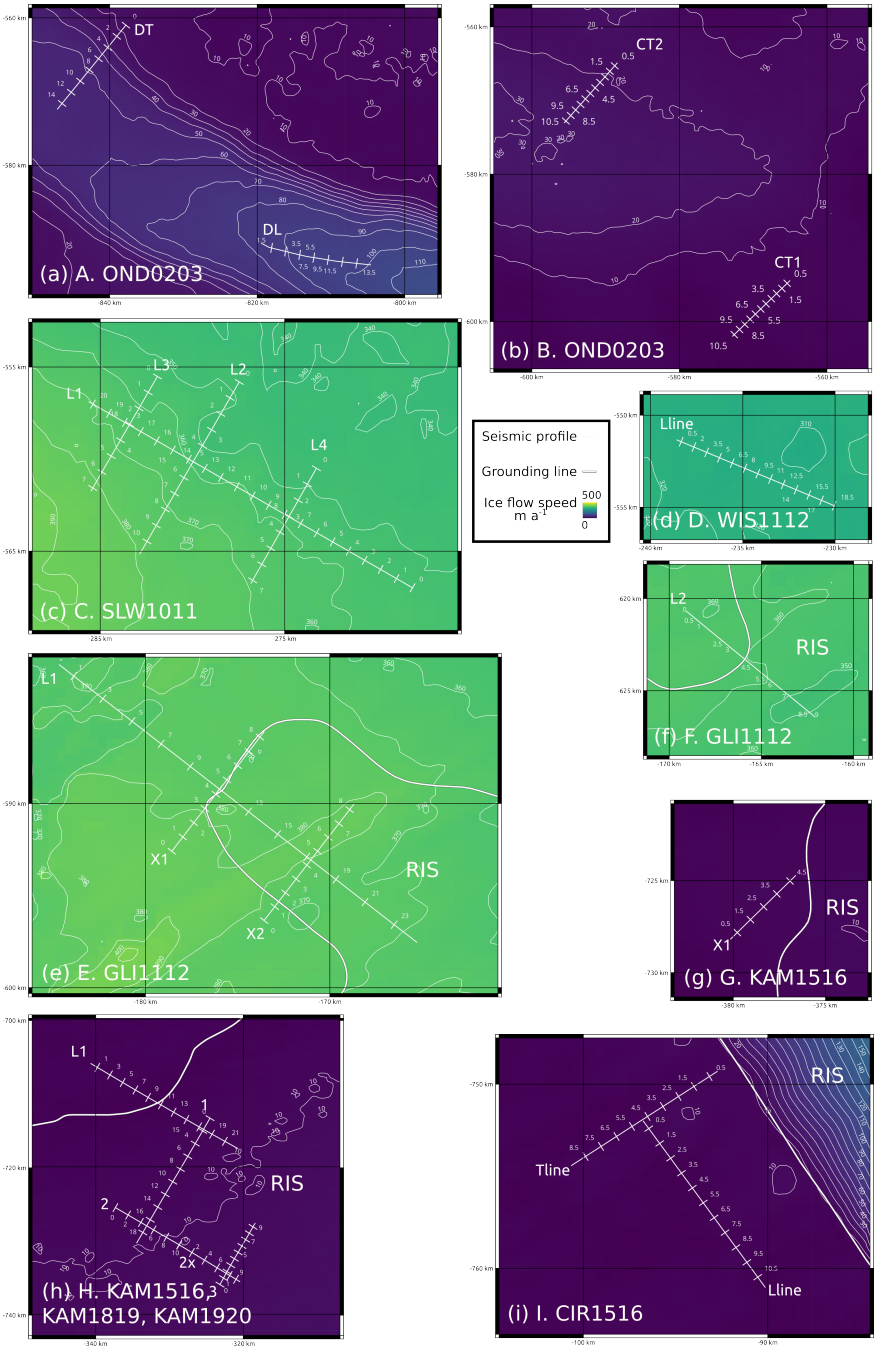


Figure 3. (a)–(i) Seismic survey locations A–I with profiles and annotated distance markers (km) shown in white. Background imagery shows ice flow velocity overlain by contours at 10 m a^{-1} intervals (Rignot et al., 2011). The grounding line separating grounded ice from the Ross Ice Shelf (RIS) is shown by the thick white line (Depoorter et al., 2013). Panels are annotated in the lower left corner with the survey name from Table 1 and location letter from Fig. 1. Seismic profiles are annotated with line names from Table 1.

https://doi.org/10.5194/essd-2026-723
Preprint. Discussion started: 2 November 2026
© Author(s) 2026. CC BY 4.0 License.



Open Access Earth System Science Data Discussions

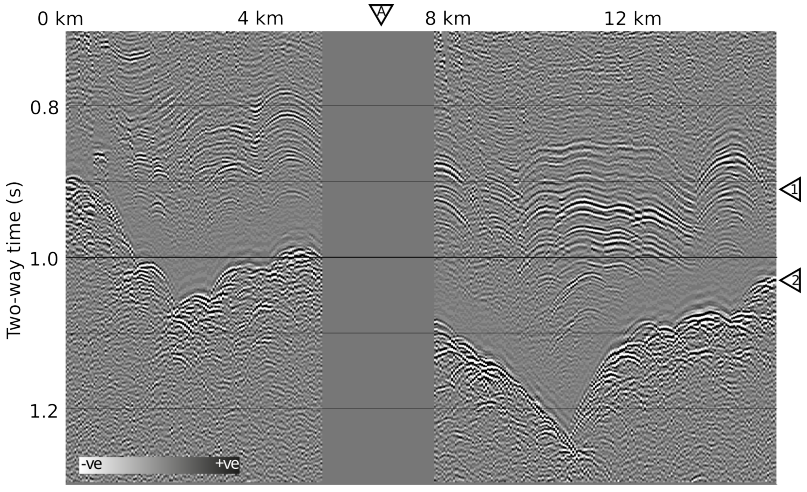


Figure 4. OND0203 line DT1 crosses the margin of Bindschadler Ice Stream in the ice stream's onset region. Slower flowing ice is on the left and faster flowing ice is on the right. Annotations mark (A) a data gap in the middle of the profile; (1) prominent englacial reflectivity reported in Horgan et al. (2011); (2) a spatially rough high-amplitude mixed-polarity bed return.

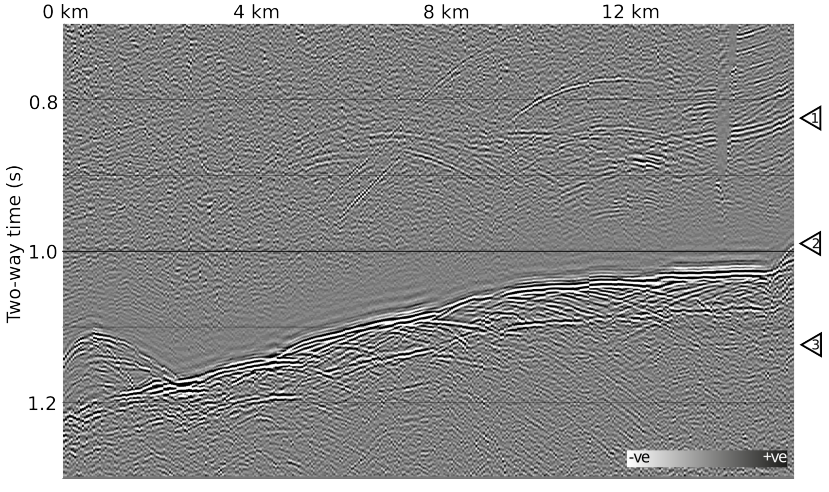


Figure 5. OND0203 line DL1 is a longitudinal profile in the centre of the onset region of Bindschadler Ice Stream. Annotations mark (1) englacial reflectivity; (2) a mostly smooth mixed-polarity bed return; (3) an apparent short-path multiple of the bed return (or of the bed ghost) of unknown origin.

https://doi.org/10.5194/essd-2026-723
Preprint. Discussion started: 2 November 2026
© Author(s) 2026. CC BY 4.0 License.



Open Access Earth System Science Data Discussions

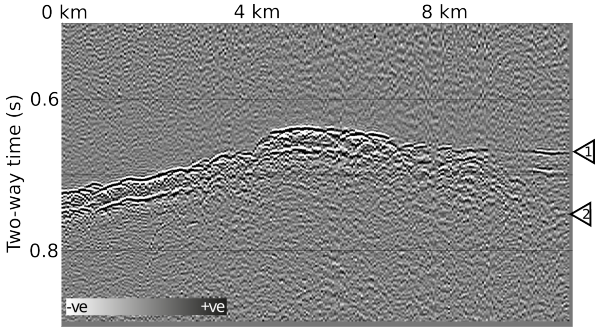


Figure 6. OND0203 line CT2 is a transverse profile upstream on Kamb Ice Stream. The profile is upstream of the stagnant ice stream trunk. The surface velocity remains low (< 30 m a^{-1}). Annotations mark (1) a mostly rough and almost entirely positive polarity basal return; (2) a deeper reflector that separates from the basal return at approximately km 9. No reflectors are discernible below the basal reflector for most of the profile (km 0–9).

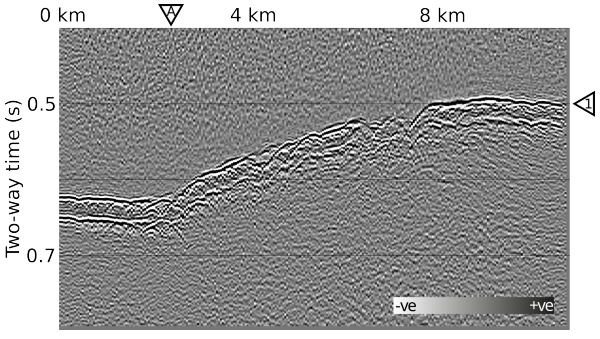


Figure 7. OND0203 line CT1 is a transverse profile that crosses a region of deflected streak lines apparent in surface imagery and elevation data. The focus of the deflections is at the right hand end of the profile. Annotations mark (1) a smooth positive polarity bed return which transitions at (A) to a rougher mostly positive polarity bed return. No reflectors are apparent below the basal reflector.

2007) and in places within the active lake boundary reflection characteristics that are not typical of an ice-water interface are observed (Figs. 8–10). Subglacial seismic returns at Lake Whillans were interpreted as a shallow lake by Horgan et al. (2012). The lake depth was interpreted to be between 0 and 8 m with a depth of approximately 8 m at the WISSARD program drilling site. Subsequent direct access encountered a 2.2 m thick water column (Tulaczyk et al., 2014), with the difference between the geophysical estimate and the drill site most likely due to lake-bed topography below the horizontal resolution of the seismic data.

Luthra et al. (2016) investigated the basal characteristics beneath a large surface feature and region of high basal drag beneath Whillans Ice Stream (Fig. 3d). The WIS1112 survey LLine (Fig. 11) shows a smooth basal reflector that is generally positive polarity with varying amplitude. Beneath the basal reflector the underlying stratigraphy is well imaged with several

https://doi.org/10.5194/essd-2026-723
Preprint. Discussion started: 2 November 2026
© Author(s) 2026. CC BY 4.0 License.

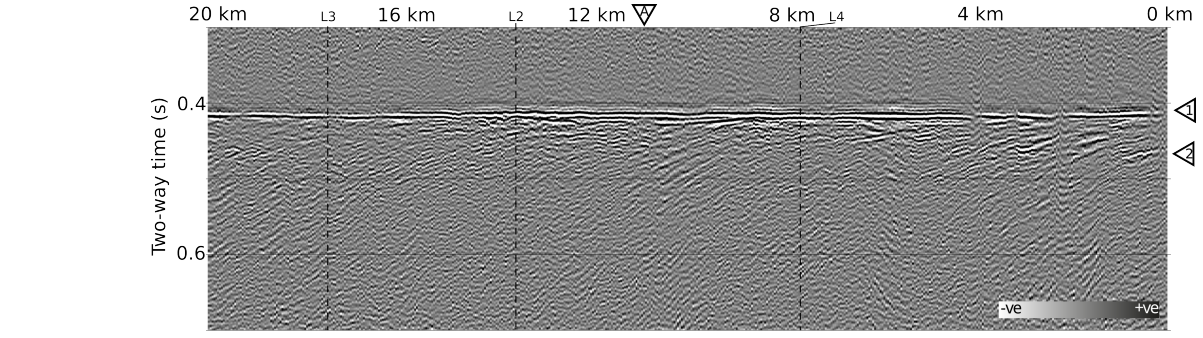


Figure 8. SLW1011 line 1 is a longitudinal profile that spans the length of Whillans Subglacial Lake. Annotations mark (A) the location of subglacial access reported in Tulaczyk et al. (2014), (1) a basal return that indicates both the presence and absence of water at the bed; (2) deeper reflectivity with an apparent upstream dip direction. The annotated dashed vertical lines denote the intersections with the transverse profiles in Figs. 9 and 10.

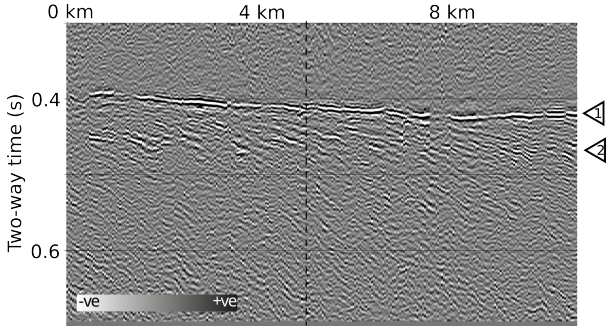


Figure 9. SLW1011 line 2 is the central transverse profile of the Whillans Subglacial Lake survey and crosses the longitudinal profile just upstream of the imaged water column. Annotations mark (1) a mixed polarity bed indicating the presence of and absence of water at the bed; (2) subglacial reflectivity with an apparent true right dip direction. The dashed vertical line denotes the intersection with the longitudinal profile in Fig. 8.

prominent subglacial reflectors overlain by generally conformable reflectivity. A region of onlapping stratigraphy is apparent at the downstream end of the profile.

3.4 Whillans Grounding Zone

125 The grounding zone of Whillans Ice Stream marks the transition between grounded ice and the floating Ross Ice Shelf (Fig. 3e, f). Upstream of the grounding zone the ice is lightly grounded, while downstream the ice overlies a thin (< 16 m) water column. Seismic profiling from the Whillans Grounding Zone survey is reported in Horgan et al. (2013, 2021), and direct access drilling in the ocean cavity was undertaken by the WISSARD program (Begeman et al., 2018, 2020). The basal return in the Whillans grounding zone shows both the high-amplitude negative-polarity return expected from ice overlying water and mixed amplitude

https://doi.org/10.5194/essd-2026-723
Preprint. Discussion started: 2 November 2026
© Author(s) 2026. CC BY 4.0 License.

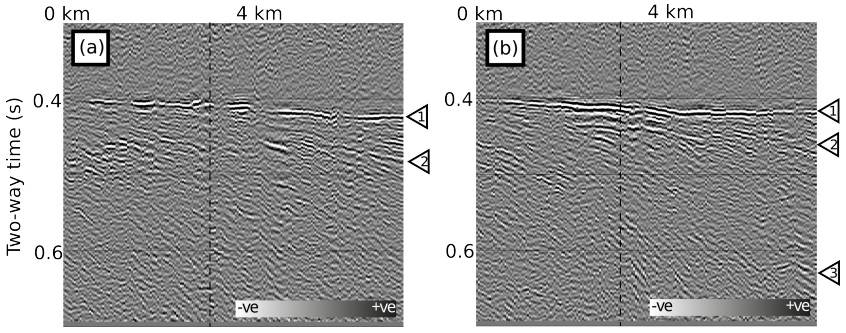


Figure 10. (a) SLW1011 line 3 is the upstream transverse profile of the Whillans Subglacial Lake survey. Annotations mark (1) the mixed polarity bed return indicating the presence and absence of water at the bed; (2) subglacial reflectivity with an apparent true right dip direction. (b) SLW1011 line 4 is the downstream transverse profile of the Whillans Subglacial Lake survey. Annotations mark (1) the mixed polarity bed return; (2) and (3) subglacial reflectivity. Dashed vertical lines in both (a) and (b) denote the intersections with the longitudinal profile in Fig. 8.

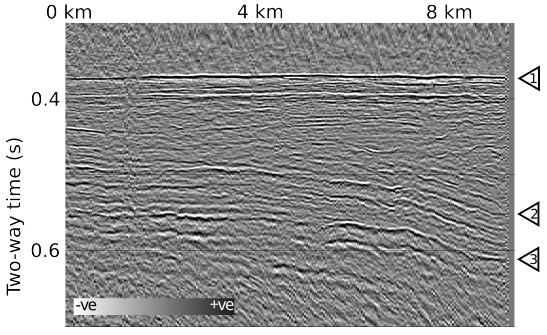


Figure 11. WIS1112 LLine is a longitudinal profile in the upper reaches of Whillans ice plain. Annotations mark (1) a smooth positive high-amplitude bed return; (2) a prominent downstream dipping subglacial reflector; (3) another prominent subglacial reflector.

and polarity returns beneath the grounded portions of the survey (Figs. 12 and 13). Isolated bodies with reflectivity indicative of water are also observed upstream of the grounding zone. Quantitative analysis of the basal return beneath grounded ice (Horgan et al., 2021) indicates stiffer subglacial material compared to that upstream at UpB (Fig. 1; Blankenship et al., 1986). Beneath the basal return laterally continuous reflectors are visible, and two prominent reflection horizons occur approximately 80–100 ms and 200–230 ms beneath the bed. These deeper reflectors form acoustic basement highs that underlie the modern grounding zone. Angular unconformities are not observed in Figs. 12 and 13, but reflectivity appears to onlap onto reflector 3 in Fig. 14.

https://doi.org/10.5194/essd-2026-723
Preprint. Discussion started: 2 November 2026
© Author(s) 2026. CC BY 4.0 License.

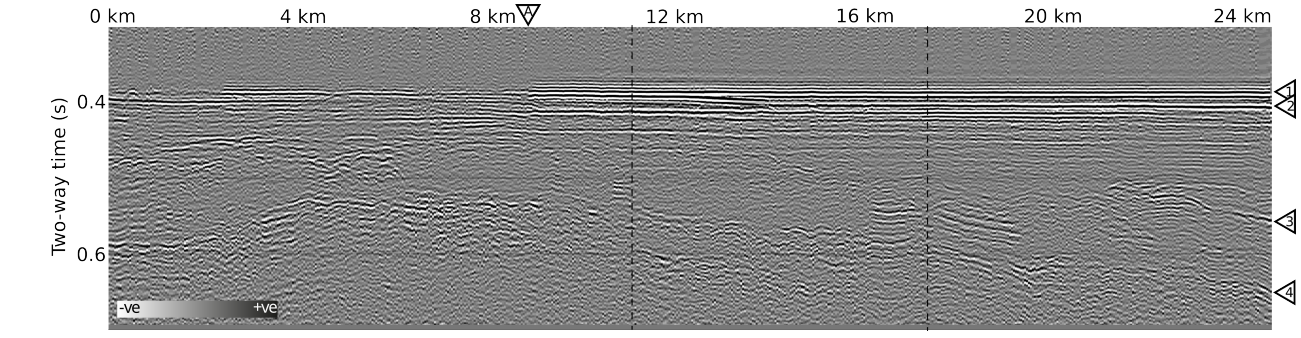


Figure 12. GLI1112 line L1 crossed from the lightly grounded Whillans ice plain to the Ross Ice Shelf. Annotations mark (1) the reflector from the base of the ice; (2) the sea bed in the sub-ice-shelf ocean cavity; (3) and (4) prominent subglacial reflectors; (A) the onset of the high-amplitude reverse-polarity reflector indicative of ice over water. Vertical dashed lines indicate the intersection with the transverse profiles shown in Fig. 13.

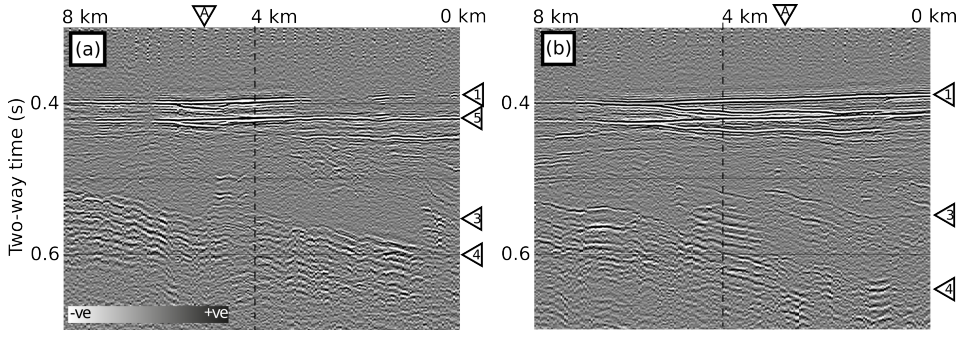


Figure 13. (a) GLI1112 line X1 is a transverse profile crossing the upstream end of Whillans Ice Stream's grounding zone embayment. Annotations mark (1) the base of the ice; (3) and (4) prominent subglacial reflectors; (5) a shallow subglacial reflector coincident with but not due to the short-path multiple; (A) a shallow and narrow water column. (b) GLI1112 line X2 is a transverse profile crossing a wider part of the embayment downstream of line X1. Annotations mark (1) the base of the ice; (3) and (4) prominent subglacial reflectors; (A) the approximate mid-point of the water column. Vertical dashed lines in (a) and (b) indicate the intersection of the transverse profiles with the longitudinal profile shown in Fig. 12.

https://doi.org/10.5194/essd-2026-723
Preprint. Discussion started: 2 November 2026
© Author(s) 2026. CC BY 4.0 License.



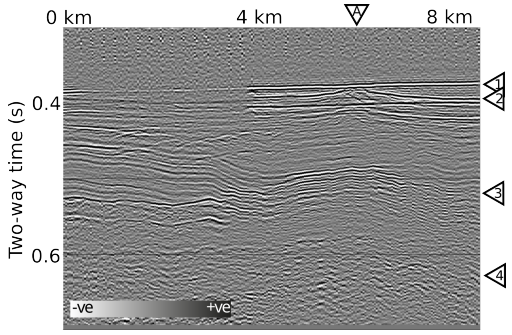


Figure 14. GLI1112 line L2 is a longitudinal profile crossing a promontory of Whillans Ice Stream (Fig. 3f). Annotations mark (1) the ice base reflector; (2) the sea-bed reflector at the base of the sub-ice-shelf ocean cavity; (3) and (4) prominent subglacial reflectors; and (A) a prominent sea-bed high that contacts the base of the ice shelf.

3.5 Kamb Ice Stream Grounding Zone

Kamb Ice Stream surveying targeted the grounding zone and sub-ice-shelf cavity (Fig. 3g, h). Surveying during the 2015–2016 season crossed a subglacial channel at the ice stream's true-right margin (Fig. 15), and crossed the grounding zone in the centre of the ice stream (Fig. 16). Surveying during the 2018–2019 and 2019–2020 seasons sought to identify an optimal subglacial drilling target beneath the thin (< 60 m) sub-ice-shelf ocean cavity (Figs. 17–19; Patterson et al. (2022)). Beneath grounded ice (Fig. 15 horizon 1 and Fig. 16 horizon 1 km 0–9) the basal reflector is faint indicating an acoustic impedance close to that of the basal ice. This weak basal reflector allows for good imaging of the underlying stratigraphy. Where the ice is afloat (Fig. 16 horizon 1 km 9–23, and Figs. 17–19 horizon 1) the basal reflector is high amplitude and negative polarity typical of ice overlying water. The base of the sub-ice-shelf ocean cavity (the sea bed) is well imaged throughout the survey (Figs. 16–19 horizon 2). The sea bed is typically smooth, with the exception of apparent roughness introduced by basal crevassing (e.g. Fig. 16 km 11–22) and a few instances of actual offsets (e.g. Fig. 19 annotation A). Subglacial reflectivity is observed consistently throughout the Kamb Ice Stream grounding zone surveys (horizon 3, Fig. 15 and horizons 3 and 4 Figs. 16–19). Subglacial reflectivity appears to be conformable at the resolution of the data with no angular truncations above or below the reflectors.

3.6 Crary Ice Rise

Ice rises are regions of grounded, slower flowing ice that can buttress the flow of faster flowing ice from upstream, thereby playing a significant role in ice dynamics (Matsuoka et al., 2015). Crary Ice Rise lies at the downstream end of Whillans Ice Stream and was the location of a subglacial drilling campaign during the 2025–2026 Antarctic season. Seismic profiling at Crary Ice Rise (Fig. 3i) is comprised of one longitudinal profile along the axis of the ice rise (Fig. 20) and one transverse line that crosses the ice rise axis (Fig. 21). The basal reflector beneath Crary Ice Rise is mostly low amplitude and difficult to

https://doi.org/10.5194/essd-2026-723
Preprint. Discussion started: 2 November 2026
© Author(s) 2026. CC BY 4.0 License.



Open Access Earth System Science Data Discussions

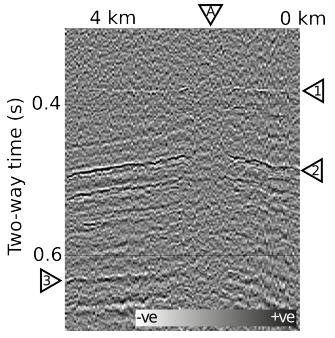


Figure 15. KAM1516 line X1 crosses a subglacial channel at the grounding zone of Kamb Ice Stream. Annotations mark (A) the location of the subglacial channel reported in Whiteford et al. (2022) and Horgan et al. (2025); (1) the ice–bed interface; (2) and (3) prominent subglacial reflectors.

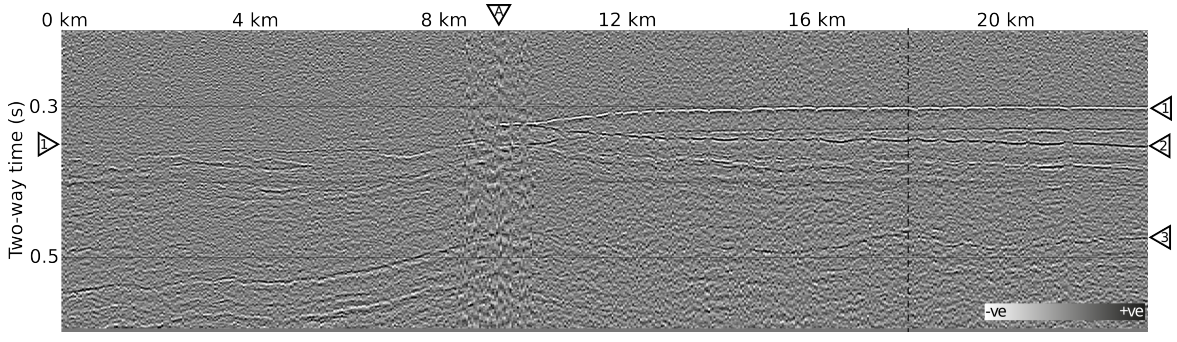


Figure 16. KAM1516 line L1 crosses the grounding zone of Kamb Ice Stream. Annotations mark (A) the first seismically detectable water at the grounding zone transition; (1) the ice–bed and ice–water interface; (2) the water–sea-bed interface; (3) a prominent subglacial and sub-sea-bed reflector which corresponds to Reflector D in Patterson et al. (2022). The dashed vertical line denotes the intersection with KAM1819 line 1 (Fig. 17).

identify in places. Horizons 1 and 2 (Figs. 20 and 21) bracket a seismic unit that reduces in thickness in the upstream and true left direction. Deeper reflectivity shows laterally continuous horizons overlying a spatially rough acoustic basement.

4 Discussion

4.1 Onset region

Seismic imaging in the onset region is broadly consistent with the conclusion that subglacial geology plays a role in the onset and position of ice streams (Bell et al., 1998; Anandakrishnan et al., 1998). Seismic profile OND0203 DT1 (Figs. 3a, 4) from Bindschadler Ice Stream shows a generally rough mixed polarity bed with no apparent underlying stratigraphy, indicating the ice is underlain by consolidated bedrock. (We note that our inability to image impedance contrasts at depth is not proof of

https://doi.org/10.5194/essd-2026-723
Preprint. Discussion started: 2 November 2026
© Author(s) 2026. CC BY 4.0 License.



Open Access Earth System Science Data Discussions

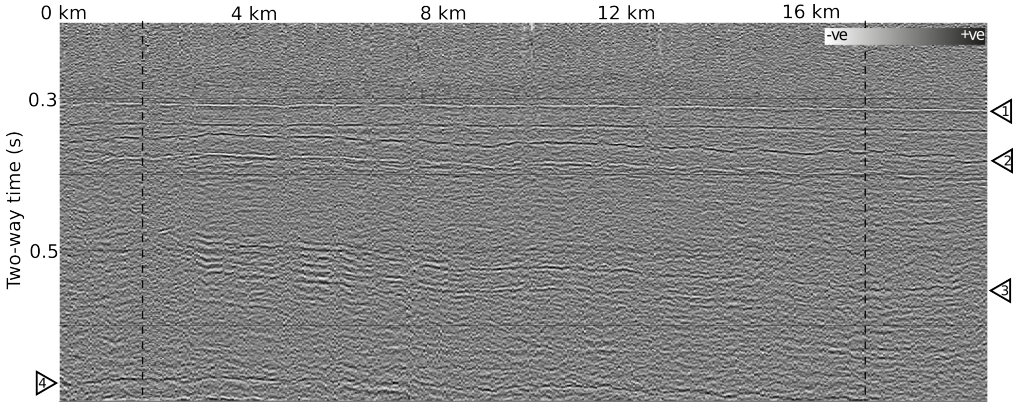


Figure 17. KAM1819 line 1 images the ocean cavity and underlying geology proximal to Kamb Ice Stream's modern grounding zone and orthogonal to KAM1516 line L1. Annotations mark (1) the ice–ocean interface; (2) the sea bed; (3) and (4) prominent sub-sea-bed reflectors. The dashed vertical lines denote the intersection with KAM1516 line L1 (left, Fig. 16) and KAM1819 line 2 (right, Fig. 18).

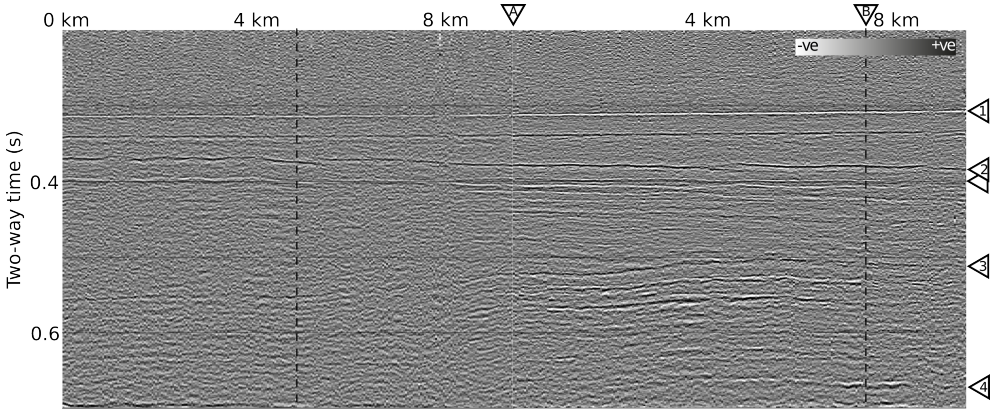


Figure 18. KAM1819 line 2 and KAM1920 line 2x extend offshore into the ocean cavity in front of Kamb Ice Stream's grounding zone. Annotations mark (A) the join between the 2018–2019 survey and the 2019–2020 survey; (B) the location of proposed palaeostratigraphic drilling; (1) the ice–ocean interface; (2) the sea bed (and conformable reflector below the sea bed); (3) and (4) prominent sub-sea-bed reflectors. Vertical dashed lines denote the intersection with KAM1819 line 1 (left, Fig. 17) and KAM1920 line 3 (right, Fig. 19).

https://doi.org/10.5194/essd-2026-723
Preprint. Discussion started: 2 November 2026
© Author(s) 2026. CC BY 4.0 License.



Open Access Earth System Science Data Discussions

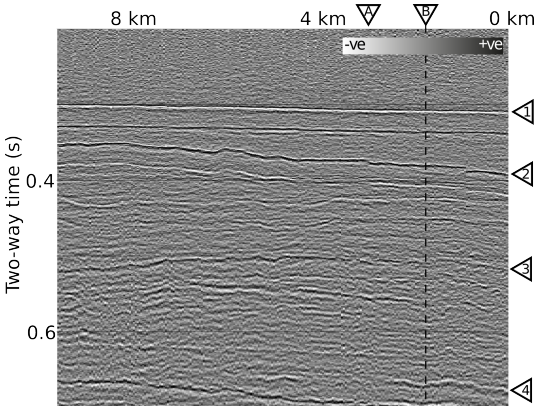


Figure 19. KAM1920 line 3 images the ocean cavity downstream of Kamb Ice Stream's grounding zone. Annotations mark (A) an example of step changes in the sea bed; (B) the location of proposed palaeostratigraphic drilling; (1) the ice–ocean interface; (2) the sea bed; (3) and (4) prominent sub-sea-bed reflectors. Vertical dashed line marks the intersection with KAM1920 line 2x.

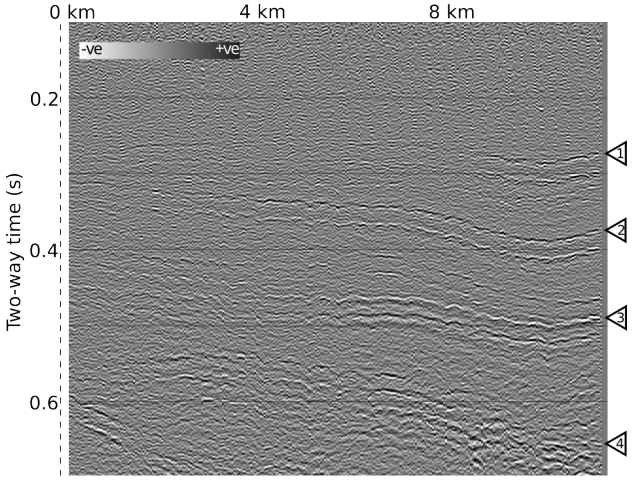


Figure 20. CIR1516 LLine is a longitudinal profile running along the crest of Crary Ice Rise. Annotations mark (1) the variable amplitude ice base reflection; (2) and (3) prominent subglacial reflectors; (4) the acoustic basement horizon. The dashed vertical line shows the projected intersection with the CIR1516 TLine.

https://doi.org/10.5194/essd-2026-723
Preprint. Discussion started: 2 November 2026
© Author(s) 2026. CC BY 4.0 License.



Open Access Earth System Science Data Discussions

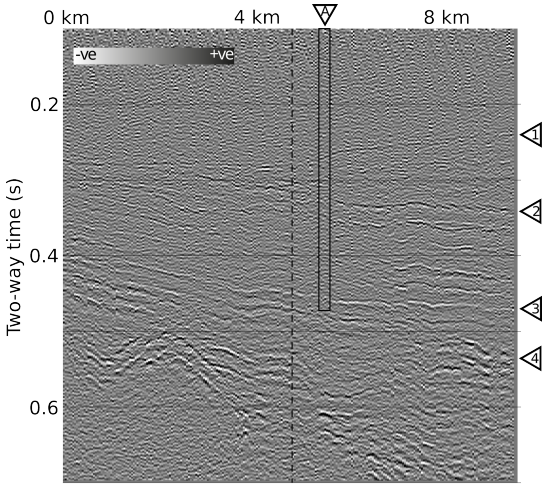


Figure 21. CIR1516 TLine is a transverse profile crossing the crest of Crary Ice Rise. Annotations mark (1) a faint ice base reflector; (2) and (3) prominent subglacial reflectors; (4) a spatially rough acoustic basement horizon. The vertical dashed line denotes the projected intersection with CIR1516 LLine. Annotation (A) and the rectangular box denote the location and approximate depth of the geological core recovered during the 2025–2026 season.

their absence.) Downstream on Bindschadler Ice Stream, where Peters et al. (2007) report extensive basal meltwater beneath profile OND0203 DL1 (Figs. 3a, 5) the bed is generally smooth with subglacial reflectivity indicating the likely presence of a sediment mantle. This is in keeping with the receiver function analysis of Anandakrishnan and Winberry (2004) which indicates a sedimentary thickness of 250 ± 50 m approximately 2.5 km from the upstream end of the profile. Beneath upper Kamb Ice Stream, OND0203 profile CT2 (Figs. 3b, 6) exhibits a generally rough bed, but the bed is smooth and a likely sedimentary deposit is evident at the faster flowing (true right) end of the profile.

4.2 Sticky spots and ice rises

Several seismic campaigns have targeted ice stream sticky spots due to their role in controlling ice stream flow (Stokes et al., 2007; Hudson et al., 2023). Profile CT1 on Kamb Ice Stream (Figs. 3b, 7) crosses an apparent sticky spot beneath the now stagnant ice. The seismic profile exhibits a smooth bed that transitions to a rougher bed. The previously faster flowing portion of the glacier (as indicated by streak lines) is underlain by a smooth bed, which appears to be either mantled by sediment and, or, smoothed by erosion. No reflectivity is observed more than a few 10s of ms below the basal return. However, receiver function analysis indicates a sedimentary thickness of 180 ± 50 m beneath the previously fast flowing portion of the profile and 0 ± 50 m at the elevated end of the profile where the rougher bed is observed (Anandakrishnan and Winberry, 2004). Luthra et al. (2017) used seismic amplitude analysis on profile CT1, showing highly variable bed conditions with softer material generally located in topographic lows.

https://doi.org/10.5194/essd-2026-723
Preprint. Discussion started: 2 November 2026
© Author(s) 2026. CC BY 4.0 License.

Open Access Earth System Science Data Discussions

The Crary Ice Rise surveys (Figs. 3i, 20 and 21) are the only seismic profiles reported here which can be directly compared to geological samples, the site having been cored to a depth of 228 m below the bed during the 2025–2026 austral summer. The temperature observations of Bindschadler et al. (1990) also provide rare constraints, indicating a temperature of -6 °C and permafrost conditions at the bed. The weak basal reflection event observed beneath Crary Ice Rise (reflector 1 in Figs. 20 and 21) would in the absence of temperature information likely be interpreted as high porosity subglacial till (e.g. Atre and Bentley, 1993), highlighting the nonuniqueness that can result when determining bed types from normal-incidence seismic observations. While detailed analysis of the CIR sedimentary core is still in progress, the seismic-based drilling prognosis presented in Patterson et al. (2022) is broadly consistent with the contrasts in lithology encountered during drilling. Notably, a thick diamict sequence corresponds to the interval between reflectors 2 and 3 in Figs. 20 and 21. Figure 21 indicates some reflectivity within this section, which may indicate varying degrees of cohesiveness within the unit, but which do not necessarily result from strong contrasts in lithology. This presents a complication when identifying drilling targets as thick diamict sections can be deposited rapidly, and do not contain the range of ice sheet states that are typically desirable in subglacial drilling targets.

4.3 Subglacial hydrology

The characteristic seismic return resulting from ice overlying water (high amplitude and negative polarity) makes active source seismology well suited to investigate some aspects of subglacial hydrology. Observations from the shallow Whillans Subglacial Lake (Fig. 8) and the grounding zone estuary of Whillans Ice Stream (Figs. 12) support this assertion with clearly delineated subglacial water confirmed by subglacial access (Tulaczyk et al., 2014; Begeman et al., 2018). Narrow and shallow targets result in more ambiguity, as observed at the subglacial channel crossing the grounding zone of Kamb Ice Stream (Fig. 15). This subglacial channel is not apparent in the seismic data despite being prominent in radar observations (Whiteford et al., 2022) and subglacial drilling encountering a large (> 100 m wide and approximately 250 m high) water filled channel (Horgan et al., 2025). Instead of imaging the top of the channel, the seismic methods show a lack of returns where the channel is present. Similarly, the discrepancy between the estimated and observed water depths in Whillans Subglacial Lake (Tulaczyk et al., 2014) highlights the need for awareness of spatial resolution when relying on seismic data to investigate thin water bodies beneath ice sheets.

4.4 Grounding zone deposition

Sediment deposition at grounding zones has been observed both in the modern system (Powell et al., 1996) and on the continental shelf surrounding Antarctica and elsewhere (e.g. Batchelor and Dowdeswell, 2015). Grounding zone deposits, typically characterised by their asymmetric wedge-shape, are frequently interpreted to mark still-stands occupied during ice sheet retreat (e.g. Bart and Owolana, 2012; Simkins et al., 2018). Sediment deposits are interpreted beneath the modern grounding zone of Whillans Ice Stream (Fig. 12), although not the characteristic wedge-like deposits observed elsewhere (Horgan et al., 2013). The modern grounding zone of Kamb Ice Stream exhibits no sediment deposits at the grounding line, leading Horgan et al. (2017) to conclude the grounding zone has retreated to its current location after the ice stream's stagnation. We note that some offsets in the sea bed (e.g. Fig. 19, annotation A) may be the result of grounding zone deposition during short lived still stands.

https://doi.org/10.5194/essd-2026-723
Preprint. Discussion started: 2 November 2026
© Author(s) 2026. CC BY 4.0 License.


Despite the lack of grounding zone wedge deposits observed in the modern system, active source seismology remains a suitable technique with which to investigate grounding zone still-stands due to the characteristic shape of the deposits, and the insights available from palaeodeposits on the continental shelf.

4.5 Ocean cavity and sub-ice-shelf deposition

Active source seismology is well suited for precise studies of bathymetry beneath ice shelves where radar methods are unsuitable and gravity methods can fail to provide the required fidelity (Brisbourne et al., 2014, 2020). Much of the bathymetry beneath the Ross Ice Shelf and Filchner–Ronne Ice Shelf relies on seismic observations (e.g. Bentley, 1990; Rosier et al., 2018). However, the utility of seismic methods for bathymetry is often limited by the effort required, making gravity derived bathymetry a pragmatic choice (e.g. Tinto et al., 2019). In cases where gravity methods are used, seismic observations provide important constraints (Tankersley et al., 2025). Seismic imaging beneath ice shelves has been effectively applied to studies from crustal-scale tectonics (ten Brink et al., 1993) to sub-ice-shelf geomorphology (Oetting et al., 2022). The sub-ice-shelf data presented here focus on the grounding zone environment, where the ocean cavity tapers to zero thickness, and much of the threshold behaviour of ice sheets is thought to reside. Both Kamb Ice Stream and Whillans Ice Stream (Figs. 12, 13, and 16–19) exhibit shallow water columns (< 70 m). Sub-sea-bed stratigraphy is well imaged at both these locations. Patterson et al. (2022) propose a palaeoclimate drilling study at the intersection of KAM1920 line 2x (Fig. 18) and KAM1920 line 3 (Fig. 19) with a target drilling depth of 200 m beneath the sea bed.

5 Conclusions

The active source seismic data presented here provide spatially sparse but valuable information from beneath the Ross Ice Streams of West Antarctica. They show that active source seismology is an effective means by which insight can be gained on ice sheet internal structure, the ice–bed interface, water beneath ice sheets, the sub-ice-shelf ocean cavity, and subglacial geology and stratigraphy. They confirm the long held view that streaming ice flow is correlated with an underlying sediment substrate, and show that much of the lower portions of the Ross Ice Streams are underlain by regionally extensive sedimentary deposits in excess of several hundred metres thick. Seismic methods are skilled at locating water in concentrated zones beneath the ice streams, although resolution limits hamper investigation of the routing of the small quantities of water produced beneath West Antarctica. Seismic observations have proved effective at locating palaeostratigraphic drilling targets beneath the ice sheets (e.g. Patterson et al., 2022). However, current methods need more skill to accurately determine subglacial lithology. This is a key consideration when locating potential drilling targets, as some lithologies (e.g. diamictite) can be deposited rapidly, resulting in the potential for drilling programs to retrieve short temporal records capturing a narrow range of ice sheet behaviour despite coring to considerable (hundreds of metres) depth. The most frequently employed seismic acquisition methods are well suited for small, relatively light weight field efforts at scales of tens of kilometres, but poorly suited to the more regional studies at scales of hundreds of kilometres. These larger scales require the efficiency provided by repeatable sources and towed receivers (e.g. the vibroseis source and snow streamers reported by Eisen et al., 2015). Future data acquisition should focus on

https://doi.org/10.5194/essd-2026-723
Preprint. Discussion started: 2 November 2026
© Author(s) 2026. CC BY 4.0 License.



expanding and, if possible, connecting the sparse surveys where palaeostratigraphic drilling efforts are focused. Such efforts promise to provide process knowledge, valuable primary data (e.g. bathymetry), and much needed insight into the past response of the ice sheets to environmental forcing.

6 Code and data availability

All data are available on Zenodo (https://doi.org/10.5281/zenodo.19068423, Horgan et al., 2026) under a CC BY-SA 4.0 copyright licence. Data are provided in the industry standard SEG-Y Revision 1 data format in both the unprocessed (shot) form and the processed (stacked) form. The complete file list is shown in Table A2.

Appendix A

A1 Seismic data processing

Seismic data processing was performed using GLOBE Claritas (https://www.globeclaritas.com; Ravens, 2001) and followed the representative workflow presented in Table A1. Raw and processed data files are listed in Table A2. Some data sets required bespoke processing steps such as static corrections to account for variable shot depths, and surgical mutes to remove noise. Some processing stages are repeated, for example, those where the velocity model is refined. Source, receiver, and common depth point (CDP) coordinates are preserved in the SEG-Y trace headers in polar stereographic (EPSG:3031) coordinates in decimetres. To plot positions in the EPSG:3031 projection the SEG-Y header values should be divided by the scalar value (10). In the shot data the source positions are present in the 240-byte trace headers in byte positions 73–76 (easting) and 77–80 (northing) and the receiver positions are present in byte positions 81–84 (easting) and 85–88 (northing). In the stacked data trace positions are present in the 240 byte trace headers in byte positions 197–200 (easting) and byte positions 201–204 (northing).

Author contributions. HJH acquired funding, led field data acquisition, processed and interpreted data, and wrote the manuscript. AG led field data acquisition, processed and interpreted data. JPW acquired funding, led field data acquisition and interpreted data. SA acquired funding, led field data acquisition and interpreted data. HC acquired funding, contributed project leadership and acquired field data. GD acquired funding and contributed project leadership. TvdF acquired funding and contributed project leadership. DK acquired funding and contributed project leadership. RL acquired funding and contributed project leadership. MP acquired funding and contributed project leadership. IS assisted with data interpretation, management and curation. All authors contributed to revision of the manuscript.

Competing interests. The authors declare that they have no competing interests.

https://doi.org/10.5194/essd-2026-723
Preprint. Discussion started: 2 November 2026
© Author(s) 2026. CC BY 4.0 License.



Open Access Earth System Science Data Discussions

Table A1. Active source seismic processing steps.

Processing step	Processing stage
Read field data	Prestack 1
Add geometry	Prestack 1
Bandpass frequency filter	Prestack 1
Edit bad traces	Prestack 1
Save and visually inspect data	Prestack 1
Read Prestack 1 data	Stack 1
Sort to Common Depth Point (CDP) gathers	Stack 1
Apply 1D normal moveout correction	Stack 1
Stack CDP traces	Stack 1
Bandpass Filter	Stack 1
Save and visually inspect data	Stack 1
Create 2D velocity model	Velocity analysis
Read Prestack 1 data	Prestack 2
Correct for spherical spreading	Prestack 2
Coherency filter	Prestack 2
Wiener deconvolution	Prestack 2
Bandpass filter	Prestack 2
Save and visually inspect data	Prestack 2
Refine 2D velocity model	Velocity analysis
Read Prestack 2 data	Stack 2
Sort to Common Depth Point (CDP) gathers	Stack 2
Apply normal moveout correction	Stack 2
Stack CDP traces	Stack 2
Save and visually inspect data	Stack 2
Refine 2D velocity model	Velocity analysis
Read Stack 2 data	Migration
Finite difference migration	Migration
Save and visually inspect data	Migration

https://doi.org/10.5194/essd-2026-723
Preprint. Discussion started: 2 November 2026
© Author(s) 2026. CC BY 4.0 License.



Open Access Earth System Science Data Discussions

Table A2. SEG-Y files.

Survey	Line	Shot file	Stack file
OND0203	CT1	ond0203_ct1_shot.segy	ond0203_ct1_stack.segy
OND0203	CT2	ond0203_ct2_shot.segy	ond0203_ct2_stack.segy
OND0203	DL1	ond0203_dl1_shot.segy	ond0203_dl1_stack.segy
OND0203	DT1	ond0203_dt1_shot.segy	ond0203_dt1_stack.segy
SLW1011	L1	slw1011_l1_shot.segy	slw1011_l1_stack.segy
SLW1011	L2	slw1011_l2_shot.segy	slw1011_l2_stack.segy
SLW1011	L3	slw1011_l3_shot.segy	slw1011_l3_stack.segy
SLW1011	L4	slw1011_l4_shot.segy	slw1011_l4_stack.segy
WIS1112	LLine	wis1112_lline_shot.segy	wis1112_lline_stack.segy
GLI1112	L1	gli1112_l1_shot.segy	gli1112_l1_stack.segy
GLI1112	X1	gli1112_x1_shot.segy	gli1112_x1_stack.segy
GLI1112	X2	gli1112_x2_shot.segy	gli1112_x2_stack.segy
GLI1112	L2	gli1112_l2_shot.segy	gli1112_l2_stack.segy
KAM1516	X1	kam1516_x1_shot.segy	kam1516_x1_stack.segy
KAM1516	L1	kam1516_l1_shot.segy	kam1516_l1_stack.segy
KAM1819	1	kam1819_1_shot.segy	kam1819_1_stack.segy
KAM1819	2	kam1819_2_shot.segy	kam1819_2_stack.segy
KAM1920	2x	kam1920_2x_shot.segy	kam1920_2x_stack.segy
KAM1920	3	kam1920_3_shot.segy	kam1920_3_stack.segy
CIR1516	TLine	cir1516_tline_shot.segy	cir1516_tline_stack.segy
CIR1516	LLine	cir1516_lline_shot.segy	cir1516_lline_stack.segy

Acknowledgements. Our thanks to Antarctica New Zealand and the United States Antarctic Program for their commitment to deep field scientific support in Antarctica that resulted in the data presented here. HJH acknowledges the Aotearoa New Zealand Antarctic Science Platform project Antarctic Ice Dynamics (ANTA1801 ASP-021-01), the NZARI-funded Aotearoa New Zealand Ross Ice Shelf Program (#2014-11), a Royal Society of New Zealand Rutherford Discovery Fellowship (RDF-VUW1602) and support from the Swiss National Science Fund (SNF grant 10006126). HC and JPW acknowledge funding from the United States National Science Foundation (NSF 1443356, NSF 1443552).

https://doi.org/10.5194/essd-2026-723
Preprint. Discussion started: 2 November 2026
© Author(s) 2026. CC BY 4.0 License.



References

Anandakrishnan, S. and Winberry, J. P.: Antarctic subglacial sedimentary layer thickness from receiver function analysis, Global and Planetary Change, 42, 167–176, https://doi.org/10.1016/j.gloplacha.2003.10.005, 2004.

Anandakrishnan, S., Blankenship, D. D., Alley, R. B., and Stoffa, P. L.: Influence of subglacial geology on the position of a West Antarctic ice stream from seismic observations, Nature, 394, 62–65, https://doi.org/10.1038/27889, 1998.

Atre, S. R. and Bentley, C. R.: Laterally varying basal conditions beneath ice Streams B and C, West Antarctica, Journal of Glaciology, 39, 507–514, https://doi.org/10.3189/S0022143000016403, 1993.

Bart, P. J. and Owolana, B.: On the duration of West Antarctic Ice Sheet grounding events in Ross Sea during the Quaternary, Quaternary Science Reviews, 47, 101–115, https://doi.org/10.1016/j.quascirev.2012.04.023, 2012.

Batchelor, C. L. and Dowdeswell, J. A.: Ice-sheet grounding-zone wedges (GZWs) on high-latitude continental margins, Marine Geology, 363, 65–92, https://doi.org/10.1016/j.margeo.2015.02.001, 2015.

Begeman, C. B., Tulaczyk, S. M., Marsh, O. J., Mikucki, J. A., Stanton, T. P., Hodson, T. O., Siegfried, M. R., Powell, R. D., Christianson, K., and King, M. A.: Ocean Stratification and Low Melt Rates at the Ross Ice Shelf Grounding Zone, Journal of Geophysical Research: Oceans, 123, 7438–7452, https://doi.org/10.1029/2018JC013987, 2018.

Begeman, C. B., Tulaczyk, S., Padman, L., King, M., Siegfried, M. R., Hodson, T. O., and Fricker, H. A.: Tidal Pressurization of the Ocean Cavity Near an Antarctic Ice Shelf Grounding Line, Journal of Geophysical Research: Oceans, 125, e2019JC015 562, https://doi.org/10.1029/2019JC015562, 2020.

Bell, R. E., Blankenship, D. D., Finn, C. A., Morse, D. L., Scambos, T. A., Brozena, J. M., and Hodge, S. M.: Influence of subglacial geology on the onset of a West Antarctic ice stream from aerogeophysical observations, Nature, 394, 58–62, https://doi.org/10.1038/27883, 1998.

Bentley, C. R.: The Ross Ice Shelf Geophysical and Glaciological Survey (RIGGS): Introduction and summary of measurements performed, in: The Ross Ice Shelf: Glaciology and Geophysics, pp. 1–20, American Geophysical Union (AGU), ISBN 978-1-118-66473-5, https://doi.org/10.1029/AR042p0001, 1990.

Bindschadler, R., Chen, X., and Vornberger, P.: The onset area of Ice Stream D, West Antarctica, Journal of Glaciology, 46, 95–101, https://doi.org/10.3189/172756500781833377, 2000.

Bindschadler, R. A., Roberts, E. P., and Iken, A.: Age of Crary Ice Rise, Antarctica, Determined from Temperature-Depth Profiles, Annals of Glaciology, 14, 13–16, https://doi.org/10.3189/S0260305500008168, 1990.

Blankenship, D. D., Bentley, C. R., Rooney, S. T., and Alley, R. B.: Seismic measurements reveal a saturated porous layer beneath an active Antarctic ice stream, Nature, 322, 54–57, https://doi.org/10.1038/322054a0, 1986.

Brisbourne, A., Kulessa, B., Hudson, T., Harrison, L., Holland, P., Luckman, A., Bevan, S., Ashmore, D., Hubbard, B., Pearce, E., White, J., Booth, A., Nicholls, K., and Smith, A.: An updated seabed bathymetry beneath Larsen C Ice Shelf, Antarctic Peninsula, Earth System Science Data, 12, 887–896, https://doi.org/10.5194/essd-12-887-2020, 2020.

Brisbourne, A. M., Smith, A. M., King, E. C., Nicholls, K. W., Holland, P. R., and Makinson, K.: Seabed topography beneath Larsen C Ice Shelf from seismic soundings, The Cryosphere, 8, 1–13, https://doi.org/10.5194/tc-8-1-2014, 2014.

Calkin, T., Dunbar, G. B., Atkins, C., Carter, A., Coenen, J. J., Eaves, S., Ginnane, C. E., Golledge, N. R., Harwood, D. M., Horgan, H. J., Hurwitz, B. C., Hulbe, C., Lawrence, J. D., Levy, R., Marschalek, J. W., Martin, A. P., Mullen, A. D., Neuhaus, S., Quartini, E., Schmidt, B. E., Stevens, C., Turnbull, J. C., Vermeesch, P., and Washam, P. M.: Recent sedimentology at the ground-

https://doi.org/10.5194/essd-2026-723
Preprint. Discussion started: 2 November 2026
© Author(s) 2026. CC BY 4.0 License.



ing zone of the Kamb Ice stream, West Antarctica and implications for ice shelf extent, Quaternary Science Reviews, 344, 108 988, https://doi.org/10.1016/j.quascirev.2024.108988, 2024.

Christianson, K., Jacobel, R. W., Horgan, H. J., Anandakrishnan, S., and Alley, R. B.: Subglacial Lake Whillans — Ice-penetrating radar and GPS observations of a shallow active reservoir beneath a West Antarctic ice stream, Earth and Planetary Science Letters, 331-332, 237–245, https://doi.org/10.1016/j.epsl.2012.03.013, 2012.

Cooper, A. K., Eittreim, S., Brink, U. T., and Zayatz, I.: Cenozoic Glacial Sequences of the Antarctic Continental Margin as Recorders of Antarctic Ice Sheet Fluctuations, in: The Antarctic Paleoenvironment: A Perspective on Global Change: Part Two, pp. 75–89, American Geophysical Union (AGU), ISBN 978-1-118-66806-1, https://doi.org/10.1002/9781118668061.ch5, 1993.

Depoorter, M. A., Bamber, J. L., Griggs, J. A., Lenaerts, J. T. M., Ligtenberg, S. R. M., van den Broeke, M. R., and Moholdt, G.: Calving fluxes and basal melt rates of Antarctic ice shelves, Nature, 502, 89–92, https://doi.org/10.1038/nature12567, 2013.

Dutton, A., Carlson, A. E., Long, A. J., Milne, G. A., Clark, P. U., DeConto, R., Horton, B. P., Rahmstorf, S., and Raymo, M. E.: Sea-level rise due to polar ice-sheet mass loss during past warm periods, Science, 349, aaa4019–aaa4019, https://doi.org/10.1126/science.aaa4019, 2015.

Eisen, O., Hofstede, C., Diez, A., Kristoffersen, Y., Lambrecht, A., Mayer, C., Blenkner, R., and Hilmarsson, S.: On-ice vibroseis and snowstreamer systems for geoscientific research, Polar Science, 9, 51–65, https://doi.org/10.1016/j.polar.2014.10.003, 2015.

Fretwell, P., Pritchard, H. D., Vaughan, D. G., Bamber, J. L., Barrand, N. E., Bell, R., Bianchi, C., Bingham, R. G., Blankenship, D. D., Casassa, G., Catania, G., Callens, D., Conway, H., Cook, A. J., Corr, H. F. J., Damaske, D., Damm, V., Ferraccioli, F., Forsberg, R., Fujita, S., Gim, Y., Gogineni, P., Griggs, J. A., Hindmarsh, R. C. A., Holmlund, P., Holt, J. W., Jacobel, R. W., Jenkins, A., Jokat, W., Jordan, T., King, E. C., Kohler, J., Krabill, W., Riger-Kusk, M., Langley, K. A., Leitchenkov, G., Leuschen, C., Luyendyk, B. P., Matsuoka, K., Mouginot, J., Nitsche, F. O., Nogi, Y., Nost, O. A., Popov, S. V., Rignot, E., Rippin, D. M., Rivera, A., Roberts, J., Ross, N., Siegert, M. J., Smith, A. M., Steinhage, D., Studinger, M., Sun, B., Tinto, B. K., Welch, B. C., Wilson, D., Young, D. A., Xiangbin, C., and Zirizzotti, A.: Bedmap2: improved ice bed, surface and thickness datasets for Antarctica, The Cryosphere, 7, 375–393, https://doi.org/10.5194/tc-7-375-2013, 2013.

Fricker, H. A., Scambos, T., Bindschadler, R., and Padman, L.: An Active Subglacial Water System in West Antarctica Mapped from Space, Science, 315, 1544–1548, https://doi.org/10.1126/science.1136897, 2007.

Goelzer, H., Huybrechts, P., Loutre, M.-F., and Fichefet, T.: Last Interglacial climate and sea-level evolution from a coupled ice sheet–climate model, Climate of the Past, 12, 2195–2213, https://doi.org/10.5194/cp-12-2195-2016, 2016.

Golledge, N. R., Clark, P. U., He, F., Dutton, A., Turney, C. S. M., Fogwill, C. J., Naish, T. R., Levy, R. H., McKay, R. M., Lowry, D. P., Bertler, N. a. N., Dunbar, G. B., and Carlson, A. E.: Retreat of the Antarctic Ice Sheet During the Last Interglaciation and Implications for Future Change, Geophysical Research Letters, 48, e2021GL094 513, https://doi.org/10.1029/2021GL094513, 2021.

Hearty, P. J., Hollin, J. T., Neumann, A. C., O'Leary, M. J., and McCulloch, M.: Global sea-level fluctuations during the Last Interglaciation (MIS 5e), Quaternary Science Reviews, 26, 2090–2112, https://doi.org/10.1016/j.quascirev.2007.06.019, 2007.

Hofstede, C., Beyer, S., Corr, H., Eisen, O., Hattermann, T., Helm, V., Neckel, N., Smith, E. C., Steinhage, D., Zeising, O., and Humbert, A.: Evidence for a grounding line fan at the onset of a basal channel under the ice shelf of Support Force Glacier, Antarctica, revealed by reflection seismics, The Cryosphere, 15, 1517–1535, https://doi.org/10.5194/tc-15-1517-2021, 2021.

Holland, C. W. and Anandakrishnan, S.: Subglacial seismic reflection strategies when source amplitude and medium attenuation are poorly known, Journal of Glaciology, 55, 931–937, https://doi.org/10.3189/002214309790152528, 2009.

https://doi.org/10.5194/essd-2026-723
Preprint. Discussion started: 2 November 2026
© Author(s) 2026. CC BY 4.0 License.



Horgan, H. J., Anandakrishnan, S., Alley, R. B., Burkett, P. G., and Peters, L. E.: Englacial seismic reflectivity: imaging crystal-orientation fabric in West Antarctica, Journal of Glaciology, 57, 639–650, https://doi.org/10.3189/002214311797409686, 2011.

Horgan, H. J., Anandakrishnan, S., Jacobel, R. W., Christianson, K., Alley, R. B., Heeszel, D. S., Picotti, S., and Walter, J. I.: Subglacial Lake Whillans — Seismic observations of a shallow active reservoir beneath a West Antarctic ice stream, Earth and Planetary Science Letters, 331-332, 201–209, https://doi.org/10.1016/j.epsl.2012.02.023, 2012.

Horgan, H. J., Christianson, K., Jacobel, R. W., Anandakrishnan, S., and Alley, R. B.: Sediment deposition at the modern grounding zone of Whillans Ice Stream, West Antarctica, Geophysical Research Letters, 40, 3934–3939, https://doi.org/10.1002/grl.50712, 2013.

Horgan, H. J., Hulbe, C., Alley, R. B., Anandakrishnan, S., Goodsell, B., Taylor-Offord, S., and Vaughan, M. J.: Poststagnation Retreat of Kamb Ice Stream's Grounding Zone, Geophysical Research Letters, 44, 9815–9822, https://doi.org/10.1002/2017GL074986, 2017.

Horgan, H. J., van Haastrecht, L., Alley, R. B., Anandakrishnan, S., Beem, L. H., Christianson, K., Muto, A., and Siegfried, M. R.: Grounding zone subglacial properties from calibrated active-source seismic methods, The Cryosphere, 15, 1863–1880, https://doi.org/10.5194/tc-15-1863-2021, 2021.

Horgan, H. J., Stewart, C., Stevens, C., Dunbar, G., Balfoort, L., Schmidt, B. E., Washam, P., Werder, M. A., Mandeno, D., Marschalek, J., Hulbe, C., Holschuh, N., Levy, R., Hurwitz, B., Jendersie, S., Johnson, K., Lawrence, J., Morgenstern, R., Mullen, A. D., Quartini, E., Sauthoff, W., Siegfried, M., Still, H., Thorpe-Loversuch, S., van de Flierdt, T., Venturelli, R., and Whiteford, A.: A West Antarctic grounding-zone environment shaped by episodic water flow, Nature Geoscience, 18, 389–395, https://doi.org/10.1038/s41561-025-01687-3, 2025.

Horgan, H. J., Gorman, A. R., Winberry, J. P., Anandakrishnan, S., Conway, H., Dunbar, G. B., van de Flierdt, T., Kulhanek, D. K., Levy, R., Patterson, M. O., and Santin, I.: Imaging the Ross Ice Streams of West Antarctica using active source seismology, https://doi.org/10.5281/zenodo.19068423, 2026.

Howat, I. M., Porter, C., Smith, B. E., Noh, M.-J., and Morin, P.: The Reference Elevation Model of Antarctica, The Cryosphere, 13, 665–674, https://doi.org/10.5194/tc-13-665-2019, 2019.

Hudson, T. S., Kufner, S. K., Brisbourne, A. M., Kendall, J. M., Smith, A. M., Alley, R. B., Arthern, R. J., and Murray, T.: Highly variable friction and slip observed at Antarctic ice stream bed, Nature Geoscience, 16, 612–618, https://doi.org/10.1038/s41561-023-01204-4, 2023.

Kapitsa, A. P., Ridley, J. K., de Q. Robin, G., Siegert, M. J., and Zotikov, I. A.: A large deep freshwater lake beneath the ice of central East Antarctica, Nature, 381, 684–686, https://doi.org/10.1038/381684a0, 1996.

Luthra, T., Anandakrishnan, S., Winberry, J. P., Alley, R. B., and Holschuh, N.: Basal characteristics of the main sticky spot on the ice plain of Whillans Ice Stream, Antarctica, Earth and Planetary Science Letters, 440, 12–19, https://doi.org/10.1016/j.epsl.2016.01.035, 2016.

Luthra, T., Peters, L. E., Anandakrishnan, S., Alley, R. B., Holschuh, N., and Smith, A. M.: Characteristics of the sticky spot of Kamb Ice Stream, West Antarctica, Journal of Geophysical Research: Earth Surface, 122, 641–653, https://doi.org/10.1002/2016JF004181, 2017.

Matsuoka, K., Hindmarsh, R. C. A., Moholdt, G., Bentley, M. J., Pritchard, H. D., Brown, J., Conway, H., Drews, R., Durand, G., Goldberg, D., Hattermann, T., Kingslake, J., Lenaerts, J. T. M., Martín, C., Mulvaney, R., Nicholls, K. W., Pattyn, F., Ross, N., Scambos, T., and Whitehouse, P. L.: Antarctic ice rises and rumples: Their properties and significance for ice-sheet dynamics and evolution, Earth-Science Reviews, 150, 724–745, https://doi.org/10.1016/j.earscirev.2015.09.004, 2015.

Miller, K. G., Kominz, M. A., Browning, J. V., Wright, J. D., Mountain, G. S., Katz, M. E., Sugarman, P. J., Cramer, B. S., Christie-Blick, N., and Pekar, S. F.: The Phanerozoic Record of Global Sea-Level Change, Science, 310, 1293–1298, https://doi.org/10.1126/science.1116412, 2005.

https://doi.org/10.5194/essd-2026-723
Preprint. Discussion started: 2 November 2026
© Author(s) 2026. CC BY 4.0 License.

Oetting, A., Smith, E. C., Arndt, J. E., Dorschel, B., Drews, R., Ehlers, T. A., Gaedicke, C., Hofstede, C., Klages, J. P., Kuhn, G., Lambrecht, A., Läufer, A., Mayer, C., Tiedemann, R., Wilhelms, F., and Eisen, O.: Geomorphology and shallow sub-sea-floor structures underneath the Ekström Ice Shelf, Antarctica, The Cryosphere, 16, 2051–2066, https://doi.org/10.5194/tc-16-2051-2022, 2022.

Otosaka, I. N., Shepherd, A., Ivins, E. R., Schlegel, N.-J., Amory, C., van den Broeke, M. R., Horwath, M., Joughin, I., King, M. D., Krinner, G., Nowicki, S., Payne, A. J., Rignot, E., Scambos, T., Simon, K. M., Smith, B. E., Sørensen, L. S., Velicogna, I., Whitehouse, P. L., A, G., Agosta, C., Ahlstrøm, A. P., Blazquez, A., Colgan, W., Engdahl, M. E., Fettweis, X., Forsberg, R., Gallée, H., Gardner, A., Gilbert, L., Gourmelen, N., Groh, A., Gunter, B. C., Harig, C., Helm, V., Khan, S. A., Kittel, C., Konrad, H., Langen, P. L., Lecavalier, B. S., Liang, C.-C., Loomis, B. D., McMillan, M., Melini, D., Mernild, S. H., Mottram, R., Mouginot, J., Nilsson, J., Noël, B., Pattle, M. E., Peltier, W. R., Pie, N., Roca, M., Sasgen, I., Save, H. V., Seo, K.-W., Scheuchl, B., Schrama, E. J. O., Schröder, L., Simonsen, S. B., Slater, T., Spada, G., Sutterley, T. C., Vishwakarma, B. D., van Wessem, J. M., Wiese, D., van der Wal, W., and Wouters, B.: Mass balance of the Greenland and Antarctic ice sheets from 1992 to 2020, Earth System Science Data, 15, 1597–1616, https://doi.org/10.5194/essd-15-1597-2023, 2023.

Patterson, M. O., Levy, R. H., Kulhanek, D. K., van de Flierdt, T., Horgan, H., Dunbar, G. B., Naish, T. R., Ash, J., Pyne, A., Mandeno, D., Winberry, P., Harwood, D. M., Florindo, F., Jimenez-Espejo, F. J., Läufer, A., Yoo, K.-C., Seki, O., Stocchi, P., Klages, J. P., Lee, J. I., Colleoni, F., Suganuma, Y., Gasson, E., Ohneiser, C., Flores, J.-A., Try, D., Kirkman, R., Koch, D., and the SWAIS 2C Science Team: Sensitivity of the West Antarctic Ice Sheet to +2°C (SWAIS 2C), Scientific Drilling, 30, 101–112, https://doi.org/10.5194/sd-30-101-2022, 2022.

Peters, L. E., Anandakrishnan, S., Alley, R. B., Winberry, J. P., Voigt, D. E., Smith, A. M., and Morse, D. L.: Subglacial sediments as a control on the onset and location of two Siple Coast ice streams, West Antarctica, Journal of Geophysical Research: Solid Earth, 111, https://doi.org/10.1029/2005JB003766, 2006.

Peters, L. E., Anandakrishnan, S., Alley, R. B., and Smith, A. M.: Extensive storage of basal meltwater in the onset region of a major West Antarctic ice stream, Geology, 35, 251–254, https://doi.org/10.1130/G23222A.1, 2007.

Peters, L. E., Anandakrishnan, S., Holland, C. W., Horgan, H. J., Blankenship, D. D., and Voigt, D. E.: Seismic detection of a subglacial lake near the South Pole, Antarctica, Geophysical Research Letters, 35, https://doi.org/10.1029/2008GL035704, 2008.

Powell, R. D., Dawber, M., McInnes, J. N., and Pyne, A. R.: Observations of the grounding-line area at a floating glacier terminus, Annals of Glaciology, 22, 217–223, https://doi.org/10.3189/1996AoG22-1-217-223, 1996.

Ravens, J.: Globe Claritas, Seismic Processing Software Manual (3rd ed.), 2001.

Rignot, E., Mouginot, J., and Scheuchl, B.: Ice Flow of the Antarctic Ice Sheet, Science, 333, 1427–1430, https://doi.org/10.1126/science.1208336, 2011.

Robin, G. d. Q. and Swithinbank, C.: Fifty years of progress in understanding ice sheets, Journal of Glaciology, 33, 33–47, https://doi.org/10.3189/S0022143000215803, 1987.

Rooney, S. T., Blankenship, D. D., Alley, R. B., and Bentley, C. R.: Till beneath ice stream B: 2. Structure and continuity, Journal of Geophysical Research: Solid Earth, 92, 8913–8920, https://doi.org/10.1029/JB092iB09p08913, 1987.

Rosier, S. H. R., Hofstede, C., Brisbourne, A. M., Hattermann, T., Nicholls, K. W., Davis, P. E. D., Anker, P. G. D., Hillenbrand, C.-D., Smith, A. M., and Corr, H. F. J.: A New Bathymetry for the Southeastern Filchner-Ronne Ice Shelf: Implications for Modern Oceanographic Processes and Glacial History, Journal of Geophysical Research: Oceans, 123, 4610–4623, https://doi.org/10.1029/2018JC013982, 2018.

Scambos, T. A., Haran, T. M., Fahnestock, M. A., Painter, T. H., and Bohlander, J.: MODIS-based Mosaic of Antarctica (MOA) data sets: Continent-wide surface morphology and snow grain size, Remote Sensing of Environment, 111, 242–257, https://doi.org/10.1016/j.rse.2006.12.020, 2007.

https://doi.org/10.5194/essd-2026-723
Preprint. Discussion started: 2 November 2026
© Author(s) 2026. CC BY 4.0 License.



Shepherd, A., Ivins, E., Rignot, E., Smith, B., van den Broeke, M., Velicogna, I., Whitehouse, P., Briggs, K., Joughin, I., Krinner, G., Nowicki, S., Payne, T., Scambos, T., Schlegel, N., A, G., Agosta, C., Ahlstrøm, A., Babonis, G., Barletta, V., Blazquez, A., Bonin, J., Csatho, B., Cullather, R., Felikson, D., Fettweis, X., Forsberg, R., Gallee, H., Gardner, A., Gilbert, L., Groh, A., Gunter, B., Hanna, E., Harig, C., Helm, V., Horvath, A., Horwath, M., Khan, S., Kjeldsen, K. K., Konrad, H., Langen, P., Lecavalier, B., Loomis, B., Luthcke, S., McMillan, M., Melini, D., Mernild, S., Mohajerani, Y., Moore, P., Mouginot, J., Moyano, G., Muir, A., Nagler, T., Nield, G., Nilsson, J., Noel, B., Otosaka, I., Pattle, M. E., Peltier, W. R., Pie, N., Rietbroek, R., Rott, H., Sandberg-Sørensen, L., Sasgen, I., Save, H., Scheuchl, B., Schrama, E., Schröder, L., Seo, K.-W., Simonsen, S., Slater, T., Spada, G., Sutterley, T., Talpe, M., Tarasov, L., van de Berg, W. J., van der Wal, W., van Wessem, M., Vishwakarma, B. D., Wiese, D., Wouters, B., and The IMBIE team: Mass balance of the Antarctic Ice Sheet from 1992 to 2017, Nature, 558, 219–222, https://doi.org/10.1038/s41586-018-0179-y, 2018.

Simkins, L. M., Greenwood, S. L., and Anderson, J. B.: Diagnosing ice sheet grounding line stability from landform morphology, The Cryosphere, 12, 2707–2726, https://doi.org/10.5194/tc-12-2707-2018, 2018.

Smith, A. M.: Subglacial bed properties from normal-incidence seismic reflection data, Journal of environmental and engineering geophysics, 12, 3–13, 2007.

Smith, B. E., Fricker, H. A., Joughin, I. R., and Tulaczyk, S.: An inventory of active subglacial lakes in Antarctica detected by ICESat (2003–2008), Journal of Glaciology, 55, 573–595, https://doi.org/10.3189/002214309789470879, 2009.

Spector, P., Stone, J., and Goehring, B.: Thickness of the divide and flank of the West Antarctic Ice Sheet through the last deglaciation, The Cryosphere, 13, 3061–3075, https://doi.org/10.5194/tc-13-3061-2019, 2019.

Stokes, C. R., Clark, C. D., Lian, O. B., and Tulaczyk, S.: Ice stream sticky spots: A review of their identification and influence beneath contemporary and palaeo-ice streams, Earth-Science Reviews, 81, 217–249, https://doi.org/10.1016/j.earscirev.2007.01.002, 2007.

Stutz, J., Eaves, S., Norton, K., Wilcken, K. M., Moore, C., McKay, R., Lowry, D., Licht, K., and Johnson, K.: Inland thinning of Byrd Glacier, Antarctica, during Ross Ice Shelf formation, Earth Surface Processes and Landforms, 48, 3363–3380, https://doi.org/10.1002/esp.5701, 2023.

Tankersley, M. D., Horgan, H., Caratori Tontini, F., and Tinto, K.: Gravity inversion for sub-ice shelf bathymetry: strengths, limitations, and insights from synthetic modeling, The Cryosphere, 19, 6827–6864, https://doi.org/10.5194/tc-19-6827-2025, 2025.

ten Brink, U. S., Bannister, S., Beaudoin, B. C., and Stern, T. A.: Geophysical Investigations of the Tectonic Boundary Between East and West Antarctica, Science, 261, 45–50, https://doi.org/10.1126/science.261.5117.45, 1993.

Tinto, K. J., Padman, L., Siddoway, C. S., Springer, S. R., Fricker, H. A., Das, I., Caratori Tontini, F., Porter, D. F., Frearson, N. P., Howard, S. L., Siegfried, M. R., Mosbeux, C., Becker, M. K., Bertinato, C., Boghosian, A., Brady, N., Burton, B. L., Chu, W., Cordero, S. I., Dhakal, T., Dong, L., Gustafson, C. D., Keeshin, S., Locke, C., Lockett, A., O'Brien, G., Spergel, J. J., Starke, S. E., Tankersley, M., Wearing, M. G., and Bell, R. E.: Ross Ice Shelf response to climate driven by the tectonic imprint on seafloor bathymetry, Nature Geoscience, 12, 441–449, https://doi.org/10.1038/s41561-019-0370-2, 2019.

Tulaczyk, S., Mikucki, J. A., Siegfried, M. R., Priscu, J. C., Barcheck, C. G., Beem, L. H., Behar, A., Burnett, J., Christner, B. C., Fisher, A. T., Fricker, H. A., Mankoff, K. D., Powell, R. D., Rack, F., Sampson, D., Scherer, R. P., Schwartz, S. Y., and Team, T. W. S.: WISSARD at Subglacial Lake Whillans, West Antarctica: scientific operations and initial observations, Annals of Glaciology, 55, 51–58, https://doi.org/10.3189/2014AoG65A009, 2014.

Whiteford, A., Horgan, H. J., Leong, W. J., and Forbes, M.: Melting and Refreezing in an Ice Shelf Basal Channel at the Grounding Line of the Kamb Ice Stream, West Antarctica, Journal of Geophysical Research: Earth Surface, 127, e2021JF006532, https://doi.org/10.1029/2021JF006532, 2022.

https://doi.org/10.5194/essd-2026-723
Preprint. Discussion started: 2 November 2026
© Author(s) 2026. CC BY 4.0 License.



Woodward, J., Smith, A. M., Ross, N., Thoma, M., Corr, H. F. J., King, E. C., King, M. A., Grosfeld, K., Tranter, M., and Siegert, M. J.: Location for direct access to subglacial Lake Ellsworth: An assessment of geophysical data and modeling, Geophysical Research Letters, 37, https://doi.org/10.1029/2010GL042884, 2010.

Zeising, O., Eisen, O., Hofstede, C., Agnew, R., Brisbourne, A., Hoffman, A. O., and Anandakrishnan, S.: Hard rocks and deep wetlands beneath Thwaites Glacier in Antarctica, Communications Earth & Environment, 7, 366, https://doi.org/10.1038/s43247-026-03502-2, 2026.